04

Modelling of three-ion ICRF heating scenario for tokamak Globus-M2

© P.A. Korepanov, N.N. Bakharev, E.Z. Gusakov, V.V. Dyachenko

Ioffe Institute, St. Petersburg, Russia
e-mail: P.Korepanov@mail.ioffe.ru

Received December 27, 2021
Revised February 22, 2022
Accepted February 23, 2022.

The goal of this paper is to assess the possibility of using a new three-ion ICRF heating scheme on the spherical tokamak Globus-M2. In the first place, the operating frequencies and positions of cyclotron harmonics were found. Matching with frequency band of RF system of Globus-M2 was made. The absorption of electromagnetic waves was modeled using a one-dimensional full-wave code. Since the appearance of high-energy particles is expected in the three-ion ICRF scheme of heating special attention is paid to a comparing the estimates for generated particles energies with their confinement in tokamak Globus-M2.

Keywords: nuclear fusion, tokamak, high temperature plasma, Globus-M, ICRF heating, three-ion ICRF, H-D-3He plasma.

DOI: 10.21883/TP.2022.05.53675.327-21

Introduction

Ion cyclotron resonance (ICR) heating has been successfully used in traditional high aspect ratio tokamaks. The main heating scenario in them is heating with a small additive of hydrogen in deuterium plasma [1–9]. From the point of view of the use of ion-cyclotron heating, tokamaks with a small aspect ratio or spherical tokamaks are placed into a separate group, the largest of which are such units as NSTX-U [10,11], MAST-U [12,13], Globus-M(2) [4,14–16], ST-40 [17,18], START [19]. The use of high-frequency methods of heating and maintaining current in them has a number of restrictions due to the properties of spherical units.

A weak magnetic field compared to traditional tokamaks (0.4 T for Globus-M) leads to the fact that the ion-cyclotron resonance frequency is in the low-frequency area (5−15 MHz). A strong change in the toroidal magnetic field during the transition from the inner to the outer wall (by a factor of 4 for the Globus-M tokamak) leads to a significant narrowing of the absorption area compared to traditional tokamaks, in which the cyclotron resonance conditions for ions are fulfilled. As a consequence, there is a weak single-pass fading effect. On the other hand, several cyclotron harmonics simultaneously fall into the tokamak cross section, which can lead to „smearing“ of the energy release over the tokamak cross section. Fig. 1 illustrates this difference.

Pioneer experiments on high-frequency ICR heating at the Globus-M tokamak ($R = 0.36$ m, $a = 0.24$ m) were carried out in the 2000s in the heating mode with a small additive of hydrogen in H−D -plasma. A doubling effect of the ion temperature was obtained at the input radio-frequency power level $P = 200$ kW [4,21–23].

In 2018, the improvement of the Globus-M tokamak was completed. At the new unit, the toroidal component of the magnetic field can be increased from 0.4 to 1 T while maintaining the same geometry and dimensions of the plasma column. Due to the increase in the toroidal magnetic field and the plasma current, a significant increase in the discharge parameters was achieved, in particular, the confinement of highspeed ions was improved [14,24]. The latter circumstance allows to discuss the application of the three-ion scenario of ion cyclotron heating of high-temperature plasma at the Globus-M2 tokamak, which has been widely discussed lately [25–27]. The fundamental concept of this scenario is to combine the cutoff condition for a fast magnetosonic (FMS) wave with the ion cyclotron resonance area for a small additive of the third ion. The blend composition of the plasma in this case should fulfil the condition [26]:

$$\min\left(\frac{Z_1}{A_1},\ \frac{Z_2}{A_2}\right) < \frac{Z_3}{A_3} < \max\left(\frac{Z_1}{A_1},\ \frac{Z_2}{A_2}\right), \qquad (1)$$

where $Z_1,\ Z_2,\ Z_3$ – is the charge number of the constituent plasma components, $A_1,\ A_2,\ A_3$ — their atomic mass, index 3 refers to ions of a small additive. This essential condition ensures that the cyclotron harmonic of the additive agent is located between the harmonics of the first and second components. In the simplest case of a hydrogen and deuterium plasma, the condition (1) takes the form

$$0.5 < \frac{Z_3}{A_3} < 1.0,$$

which only ^{3}He ions can fulfil as a small third additive. Usually, in the implementation of the three-ion scenario, plasma H−D−(^{3}He) is used, where ^{3}He is a small additive with a concentration of approximately 1%. Examples of another plasma composition can be found in [25,26].

A characteristic feature of the H−D−(^{3}He) scenario is the high specific radio-frequency power per resonant

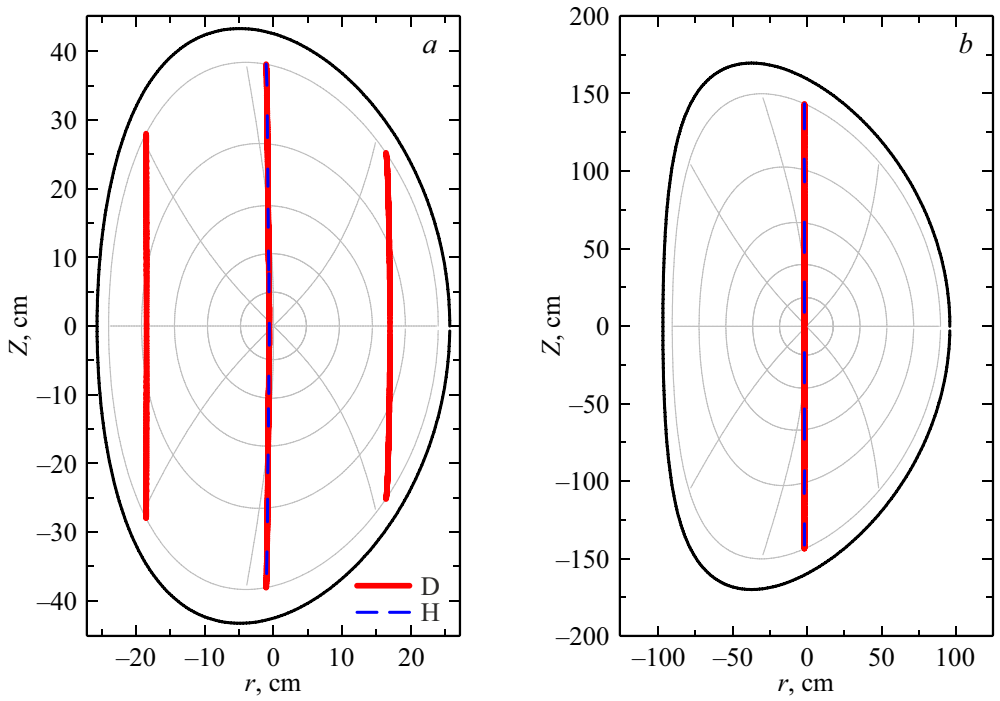

Figure 1. Comparison of the arrangement of cyclotron harmonics in a spherical tokamak (*a*) (Globus-M2 for a frequency of 11 MHz and a field of 0.7 T) and a conventional tokamak (*b*) with a large aspect ratio (standard parameters for JET [20] are used, figure for frequency 49 MHz) for hydrogen and deuterium plasma in the heating mode with a small additive of hydrogen. Solid lines (red — in the online version) — cyclotron harmonics of deuterium are specified, dashed lines (blue lines in the online version) — cyclotron harmonics of hydrogen.

particle ^{3}He. As a consequence — 3He ions obtain high energies in this scenario, which allows to simulate the retention of α-particles formed as a result of the thermonuclear reaction of deuterium and tritium in the reactor plasma [26,27].

In this paper, the opportunity of using the three-ion ICR scenario for additional plasma heating at the Globus-M2 tokamak is studied. In Section 1, the choice of operating frequencies is made and the results of modeling the propagation and absorption of electromagnetic waves in the tokamak plasma are shown. In Section 2, estimates of the energy of generated highspeed ions and calculations of their confinement are given.

1. Modeling the propagation and absorption of fast magnetosonic waves in the plasma of the Globus-M2 tokamak

In a two-component H–D plasma, there is a FMS wave cutoff area (L-cutoff) adjacent to the ion-ion hybrid layer, which arise at hydrogen concentrations above the critical value and are located between the surfaces on which the ion cyclotron resonance condition is fulfilled for hydrogen and deuterium. They appear from the side of the high field from the cyclotron harmonic of hydrogen and, as the hydrogen concentration increases, they shift towards the fundamental cyclotron harmonic of deuterium [1-3,26,28-30]. When ions of the third kind are added to the component composition of the plasma, the conditions corresponding to the harmonics of the ion cyclotron resonance of the added additive agent are fulfilled in the cross section of the plasma of a spherical tokamak. In the three-component plasma H–D–(^{3}He), the fundamental cyclotron harmonic ^{3}He is located between the first harmonics of hydrogen and deuterium due to the condition (1).

To implement the three-ion scenario, it is required to choose the ratio of the concentrations of hydrogen and deuterium in the H–D plasma in such a way as to match the cutoff position of the FMS wave for the two-component H–D plasma with the position of the cyclotron resonance ^{3}He [26]. In the paper [26] this ratio was $\sim 67\% : 33\%$, but the absorption efficiency, according to the modelling, remains within the range of hydrogen concentration from 65 to 72%. The optimal partial hydrogen concentration $X[\mathrm{H}]$ can be found as follows [26]:

$$X[\mathrm{D}] = \frac{Z_3/A_3 - Z_2/A_2}{Z_1/A_1 - Z_2/A_2} - \frac{(Z_1/A_1 - Z_3/A_3)(Z_3/A_3 - Z_2/A_2)}{(Z_1/A_1 - Z_2/A_2)}\alpha,$$

$$X[\mathrm{H}] = 1 - X[\mathrm{D}],$$

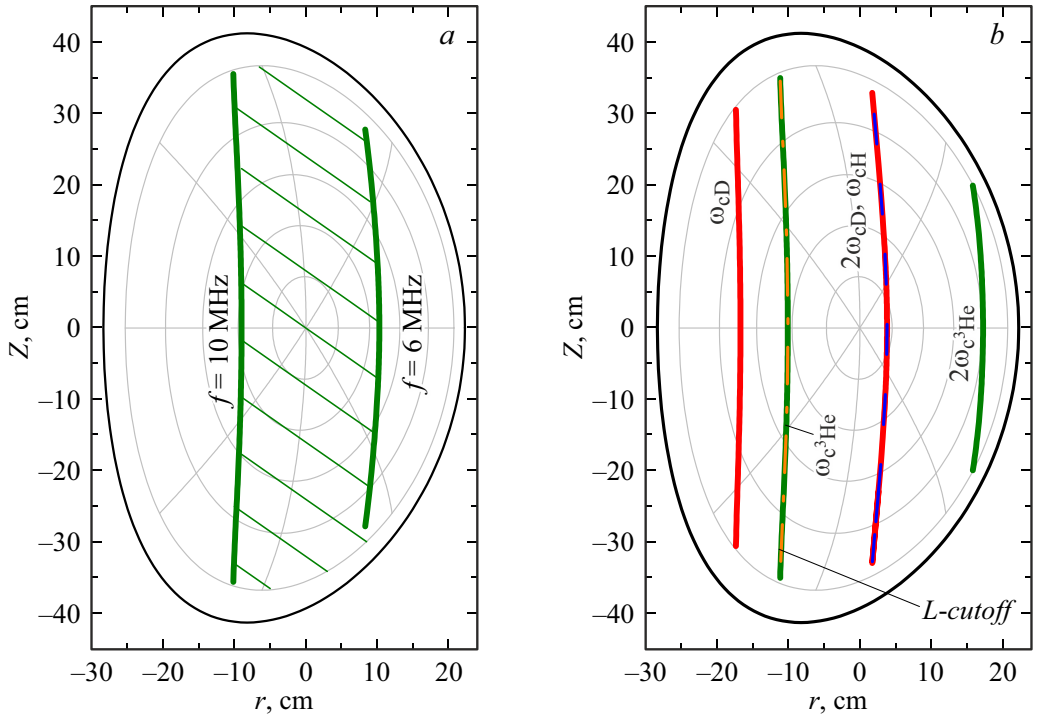

Figure 2. *a* — accessible area in the tokamak cross section, where the ^{3}He cyclotron layer can be placed; *b* — the appearance of the second harmonic of ^{3}He ions at the frequency $f = 10$ MHz from the side of a weak magnetic field near the antenna, the toroidal magnetic field on the axis of the tokamak $b_0 = 0.7$ T. Red marks the cyclotron harmonics of deuterium, blue (dashed line) — hydrogen, green — helium-3, orange (dash-dotted line) — cutoff area.

where $\alpha = \left(\frac{\omega_{cH} n_{\parallel}}{\omega_{pH}}\right)^2$, $\omega_{pH} = \left(\frac{4\pi n_e e^2}{m_H}\right)^{0.5}$. In this formula, the second term, which is proportional to the square of the ratio of the longitudinal refraction index of the FMS wave and the Alfvan refraction index under the conditions of experiments on tokamaks, is, as a rule, small.

Up to this small correction, the optimal hydrogen concentration is determined by the parameters of hydrogen and deuterium ions and does not depend on the parameters specific to the unit. The small parameter α is 0.038 for Globus-M2 and contributes about 0.1% to the partial concentration of hydrogen or deuterium.

The position of ion-cyclotron resonances is determined by the magnetic field value. For Globus-M2, the main operating field is (0.7−0.8) T in the center of the chamber. On the other hand, the position of the resonances (and the area of energy release) should be optimal for heating and confining the introduced energy: as a rule, these are the central areas of the plasma column. To improve the experiment, it is also important to be able to tune the high frequency (HF) generator in frequency The operating frequency band of the existing HF generator is $(5 - 15)$ MHz.

The area in which the helium-3 cyclotron layer can be located under the conditions of the Globus-M2 setup is shown in Fig. 2 and is limited by the available frequency band.

At a frequency of $f = 10$ MHz, the second hydrogen harmonic appears near the antenna from the side of a weak magnetic field, which can shield the central areas of the plasma, absorbing part of the high frequency power at the periphery of the discharge.

For modeling of the absorption of electromagnetic waves in a tokamak, the basic operating parameters of the discharge were used. Toroidal magnetic field on the tokamak axis $B_0 = 0.7$ T, electron density at the center $n_{e0} = 0.5 \cdot 10^{20}$ m^{-3}, current plasma $I_{\text{plsm}} = 300$ kA, electron and ion temperatures at the center $T_{e0} = 600$ eV, $T_{i0} = 300$ eV. Relative fractions of ions that make up the plasma, $X[\text{H}] = 66\%$, $X[\text{D}] = 32\%$, $X[^3\text{He}] = 2\%$. Concentration and temperature profiles selected from experimental data on the Globus-M [31] unit. The calculations were carried out using a one-dimensional full-wave code that solves Maxwell's equations in a magnetized plasma, developed at the Ioffe Physicotechnical Institute. A.F. Ioffe [22], by analogy with the works [30,32].

Modeling was carried out for two characteristic locations of cyclotron harmonics (Fig. 3), designated as A and B. In case A, the frequency 9 MHz is selected so that the first cyclotron harmonic of hydrogen is also present in the tokamak plasma, the region in which radio-frequency energy is absorbed in the classical scheme of heating with a small addition of hydrogen. In the poloidal cross section, therefore, there are simultaneously two cyclotron harmonics, at which effective absorption can be expected. In case B, the choice of the oscillator frequency 7 MHz is determined

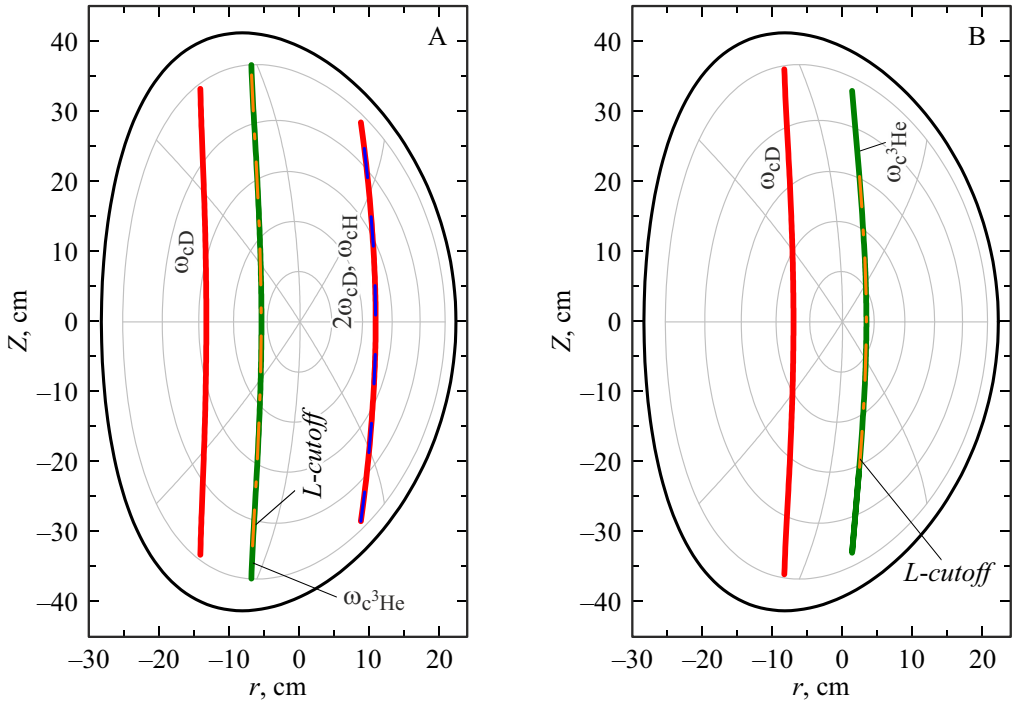

Figure 3. Location of cyclotron harmonics for options A — 9 MHz and B —7 MHz. Red marks the cyclotron harmonics of deuterium, blue (dashed line) — hydrogen, green — helium-3, orange (dash-dotted line) — cutoff area.

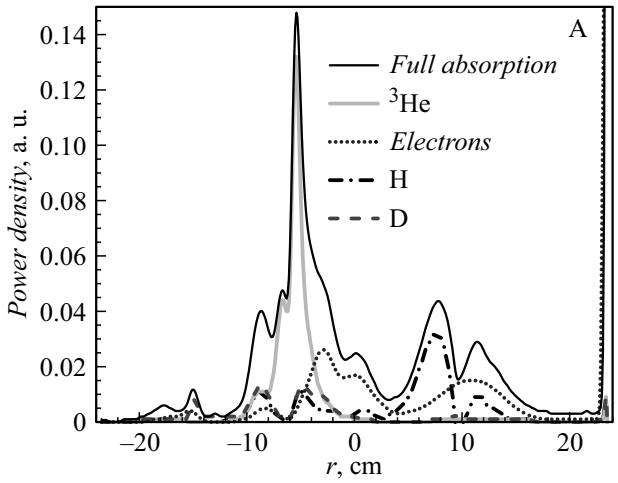

Figure 4. Distribution of absorbed power in the tokamak cross section for variant A.

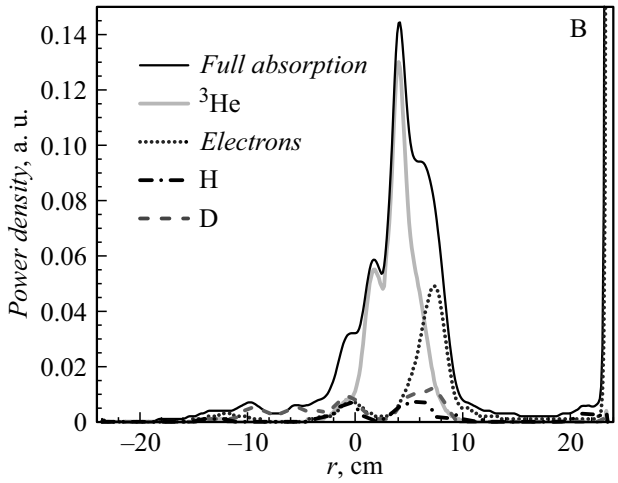

Figure 5. Distribution of absorbed power in the tokamak cross section for variant B

by the fact that only the cyclotron harmonic ^{3}He, which is located as close as possible to the tokamak axis, remains in the poloidal cross section.

The modeling results are shown in Fig. 4 and 5. The distribution of the absorbed power along the long radius of the tokamak is shown. The helium-3 cyclotron harmonic is the most efficient channel for the absorption of high frequency waves under these conditions.

As the table shows, the appearance of a cyclotron resonance of hydrogen in the plasma cross section at a frequency of 9 MHz leads to a redistribution of part of the input energy in favor of hydrogen ions.

2. Assessment of the energy of helium-3 ions

The ion energy was assessed using the theoretical model developed by Stix [33], which is also well described in [1], tested on a unit such as PLT [1,34] and gives good results congruent with experimental data. It allows to obtain

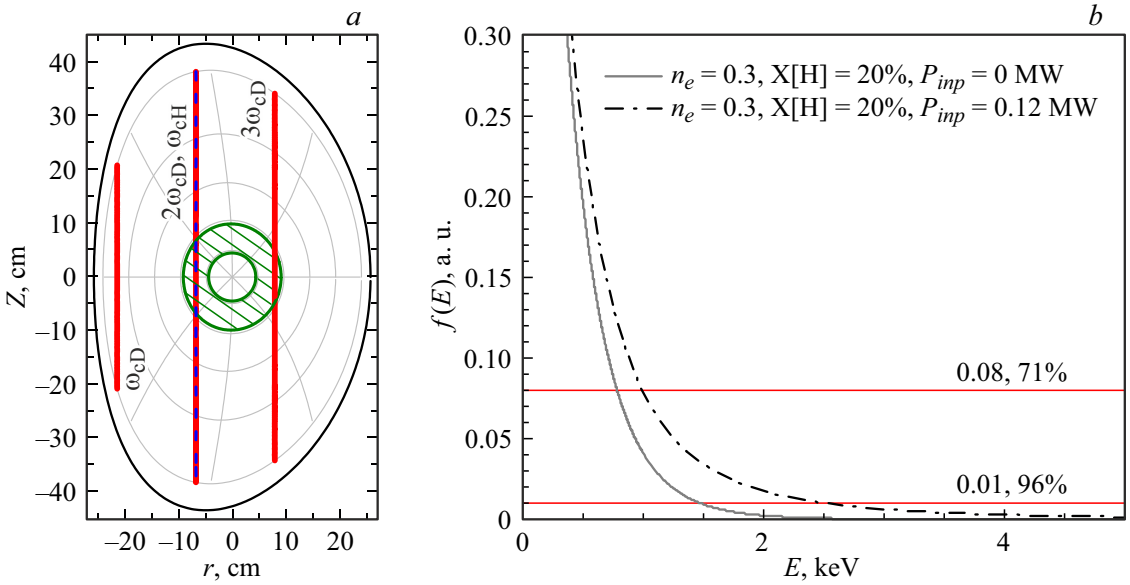

Figure 6. *a* — arrangement of cyclotron harmonics in the poloidal section of the Globus-M tokamak for the heating scenario with a small additive of hydrogen, the shaded area — the area ΔS (see (6)); *b* — hydrogen ion distribution function calculated by the model (2) for the given case: $X[\mathrm{H}] = 20\%$, $n_e = 0.3 \cdot 10^{20}\,\mathrm{m}^{-3}$, $P_{input} = 0.12\,\mathrm{MW}$. The horizontal lines mark the distribution function levels of 0.01 and 0.08, corresponding to 96% and 71% of the particle content up to the marked level.

Distribution of absorbed power by particle types

Version	f, MHz	e^-	Ions	^{3}He	H	D
A	9	45%	55%	23%	22%	10%
B	7	35%	65%	48%	6%	11%

the distribution function of particles of a small additive in plasma (2)–(4):

$$\ln f(v) = -\frac{E}{(T_e(1+\xi)}\left[1+\frac{R_f(T_e-T_f+\xi T_e)}{T_f(1+R_f+\xi)}H\left(\frac{E}{E_f}\right)\right], \tag{2}$$

$$\xi = \frac{m\langle P_\perp\rangle}{8\pi^{1/2}n_e n Z^2 e^4 \ln(\Lambda)}\left(\frac{2T_e}{m_e}\right)^{1/2}, \tag{3}$$

$$R_f = \frac{n_f Z_f^2 l_f}{n_e l_e}, \quad E_f = \frac{mT_f}{m_f}\left[\frac{3\sqrt{\pi}}{4}\frac{(1+R_f+\xi)}{1+\xi}\right]^{\frac{2}{3}},$$

$$l_f = \frac{1}{\sqrt{2}v_{T_f}}, \quad l_e = \frac{1}{\sqrt{2}v_{T_e}}, \quad E = \frac{mv^2}{2},$$

$$H(x) = \frac{1}{x}\int_0^x \frac{du}{1+u^{3/2}}. \tag{4}$$

The inferior index f denotes that the quantity $(T_f,\ n_f,\ m_f)$ belongs to background plasma ions; quantities without index $(n,\ m)$ refer to test particles, i.e. e. to ions with a small additive (^{3}He). Parameter $\langle P_\perp\rangle$ — power deposited per unit volume of plasma on the magnetic surface as a result of absorption in cyclotron resonance, λ — Coulomb logarithm, e – - electron charge, Z — charge number of test particles.

The main parameter describing the action of the electromagnetic field — ξ, characterizes the energy absorbed in cyclotron resonance per particle. In this case, this value (5) was assessed based on the power deposited in a volume of thickness Δr near a magnetic surface of small radius r, the toroidal section of which is shown in Fig. 6, 7 (6). The coefficient $k_{\%f}$ was introduced in order to take into account the distribution of the input power over the plasma components, based on the modeling results (see the table).

$$\langle P_{RF}\rangle = P_{input} \cdot k_{\%f}\Delta V, \tag{5}$$

$$\Delta V = \Delta S \cdot 2\pi R_0, \qquad \Delta S = 2\pi r \Delta r. \tag{6}$$

Figure 6 shows the calculation of the distribution function for the case of heating with a small additive of hydrogen at an input power of 0.12 MW, corresponding to the experiment published in [4,21–23], where the fraction of hydrogen $X[\mathrm{H}]$ in the component composition of the plasma varied in the band from 10 to 60%. The values of the distribution function 0.01 and 0.08 and the corresponding content of particles are marked by the red (horizontal) lines. Accordingly, the part of the distribution function with energy less than 10 keV contains up to approximately 96% of particles, and with energy less than 2 keV — up to 71%.

An ACORD-12 [35] device was used in the paper [22] to analyze the temperature and energies of the ions. The flux of hydrogen and deuterium atoms from the tokamak plasma was measured in the energy band from 0.5 to 5 keV. The effective temperature „of the tail“ piece of the distribution function was estimated tailpiece to compare

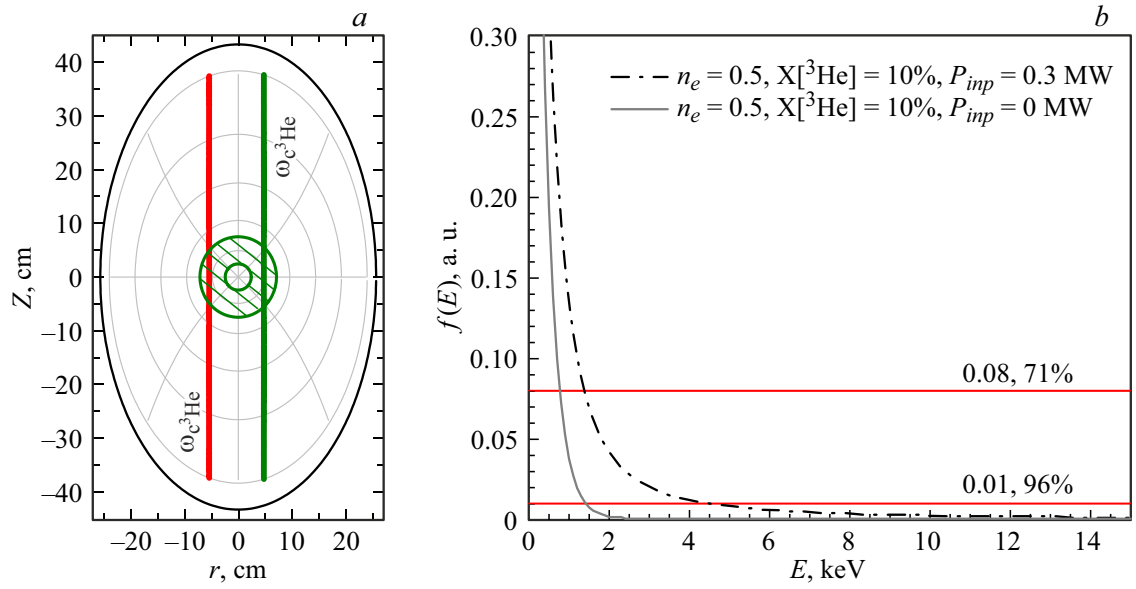

Figure 7. *a* — arrangement of cyclotron harmonics in the poloidal section of the Globus-M tokamak for the three-ion heating scenario, the shaded area corresponds to the area ΔS (see (6)); *b* — ^{3}He ion distribution function calculated by the model (2) for the given case: $X[^3\mathrm{He}] = 10\%$, $n_e = 0.5 \cdot 10^{20}\,\mathrm{m}^{-3}$, $P_{input} = 0.3\,\mathrm{MW}$. The horizontal lines mark the distribution function levels of 0.01 and 0.08, corresponding to 96% and 71% of the particle content up to the marked level.

experimental data and calculation. Assessment of the temperature „of the tail“ of hydrogen ions in the discharge №11363 [22] with parameters $n_e(0) = 3 \cdot 10^{19}\,\mathrm{m}^{-3}$, C[H] = 20%, $P_{inp} = 0.12\,\mathrm{MW}$, $f = 7.5\,\mathrm{MHz}$ was 1.13 keV, while according to the data analyzer for this discharge, the temperature „of the tail“ piece of the distribution function — 980 eV.

A similar analysis was also performed for the three-ion heating scenario (Fig. 7) in order to assess the order of expected energies in case of being used in the Globus-M2 unit and compare with particle retention data (Fig. 9). ^{3}He particles are heavier than hydrogen particles, as a result of which the distribution function for the same input power of 300 kW is more strongly pressed to the horizontal axis (Fig. 7).

Figure 8 shows diagrams that allow to assess the expected energy level of highspeed particles generated as a result of cyclotron heating. The value corresponding to the content, according to the distribution function, of 71% of particles up to the specified level is used as the expected energy level. Thus, the energy level is plotted along the vertical axis, at which, minimum 71% of the particles have energies less than the dormant one, according to (2).

Figure 9 shows the results of modeling the retention of helium-3 particles in the Globus-M2 tokamak. The equation of motion of charged particles in a magnetic field reconstructed using the EFIT code was solved numerically. The coordinates (R, Z) in the figure denote the ion „birth“,which in this case coincides with the point of reflection on the ion orbit, i.e., in the initial position at the point (R, Z), the ion has zero longitudinal velocity, and all the energy is considered to be contained in the cross stream velocity component [24]. Then the motion of the particle is modelled. The color map indicates the areas in which an ion with an energy less than the specified one is retained, and with a higher energy — it is lost. The typical energy with which the ion can still be retained in the plasma is 80 keV.

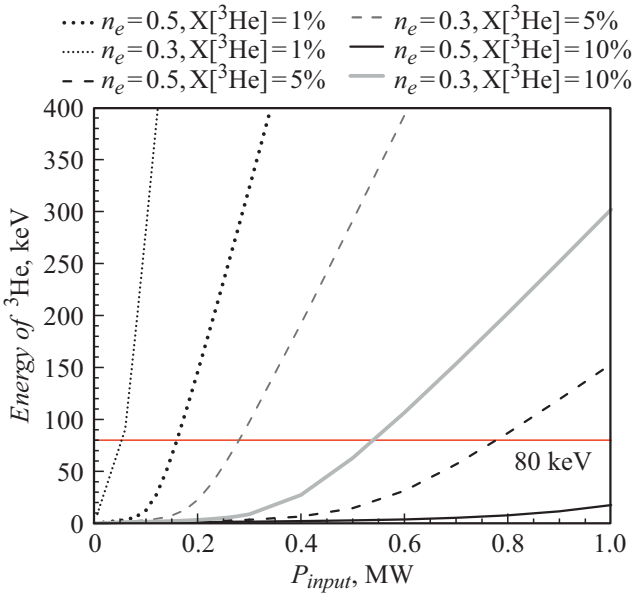

Figure 8. Dependence of the ion energy ^{3}He on the input power. The energy level is plotted along the vertical axis, at which, according to the particle distribution function, minimum 71% of the particles have energies less than the dormant one. The diagrams are given for electron densities $n_e = 0.3 \cdot 10^{20}$ and $0.5 \cdot 10^{20}\,\mathrm{m}^{-3}$.

To compare the energy range of the retained ions with the expected energies of the ^{3}He particles, diagrams are plotted in Fig. 10. On the vertical axis, the percentage of particles with energies less than 80 keV is plotted according to the distribution function depending on the input power. It can be seen from the above diagram that at partial concentrations of 3He of approximately 1% and less, most of the particles obtain an energy above 80 keV and are

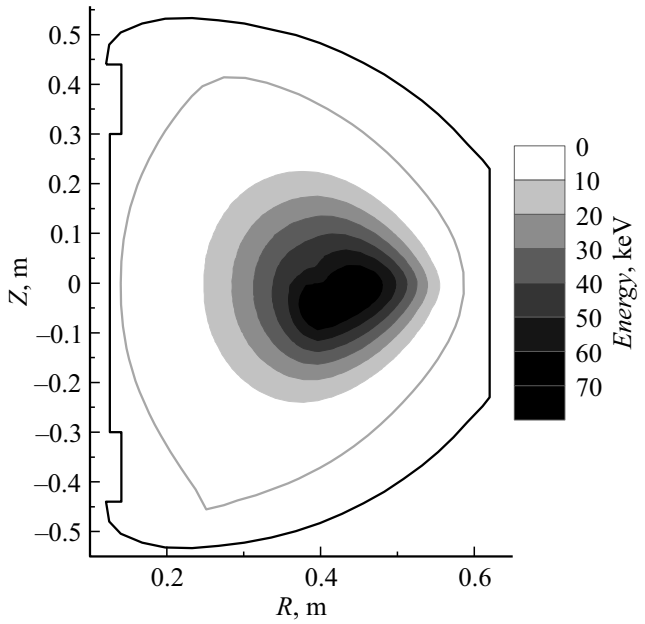

Figure 9. Modeling results of helium-3 ion confinement in the Globus-M2 unit with magnetic field $B_{tor} = 0.7$ T and plasma current $I_{plsm} = 300$ kA for discharge №37902. The maximum energy of the retained particles is 80 keV.

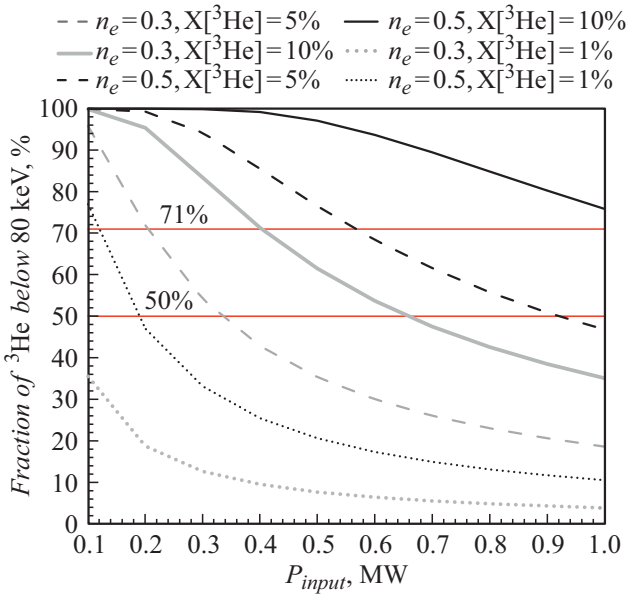

Figure 10. Dependence of the fraction of retained particles (with energy less than 80 keV) ^{3}He on the input power for electron densities is $n_e = 0.3 \cdot 10^{20}$ and $0.5 \cdot 10^{20}$ m^{-3}.

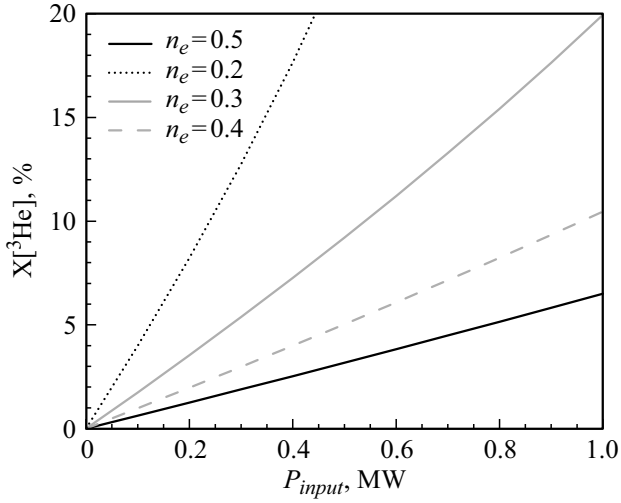

Figure 11. The partial concentration ^{3}He required for the fraction of accelerated particles with energies less than 80 keV to be 71% depending on the pumping power. Electron densities $n_e = (0.2 - 0.5) \cdot 10^{20}$ m^{-3}.

not retained in Globus-M2. With an electron density $n_e = 0.5 \cdot 10^{20}$ m^{-3} and a fraction of ^{3}He of approximately 1%, with an input power corresponding to the previous experiment [4], in 0.2–0.3 MW only 35 to 50% of the particles can be retained in the unit. And with an increase in power to 0.5 MW or more, this fraction decreases below 20%.

Due to the small size of the unit and the high energy density per particle at low partial concentrations of ^{3}He, the particles ^{3}He in their bulk obtain high energies of more than 80 keV and are not retained in the tokamak plasma. Even the most optimistic variant with electron density $n_e = 0.5 \cdot 10^{20}$ m^{-3} at partial concentrations of 1% gives only 35–50% of retained particles (Fig. 10). Therefore, for such small $X[^3\text{He}]$ as 1%, which are required for a full-scale three-ion scenario H–D–(^{3}He), it is impossible to expect with a guarantee the pronounced heating effect.

As the partial concentrations of ^{3}He increase, the situation improves. Concentrations of 5% are sufficient (Fig. 10, $n_e = 0.5 \cdot 10^{20}$ m^{-3}, $X[^3\text{He}] = 5\%$) in order for a large fraction of particles to fall into the retained energy range up to 80 keV, although the proposed three-ion heating scenario requires small partial concentrations of the third component (less than 1%), since at increasing As $X[^3\text{He}]$, the resonant polarization leading to effective wave absorption decreases. When heating with a small additive of hydrogen, the requirements for the partial concentration of hydrogen are similar: $X[\text{H}] \approx 0.1\%$, however, in experiments on the Globus-M [4] spherical tokamak, the heating effect was preserved at partial concentrations of hydrogen from 10 to 60%. This circumstance allows to expect that the same effect can take place in the case of H–D–(^{3}He).

In order to demonstrate more clearly what partial concentrations of ^{3}He are required for efficient retention of

the generated highspeed ions, the diagrams in Fig. 11 are shown. The fraction of ^{3}He is plotted along the vertical axis, above which in the band of retained energies 0−80 keV, according to (2), it turned out to be minimum 71% of particles. As can be seen, for this at an electron density of $n_e = 0.5 \cdot 10^{20}\,\mathrm{m}^{-3}$ for pumping powers available on Globus-M2 not exceeding 1 MW , $X[^3\mathrm{He}]$ it should be minimum 7%, and for a power of 0.3 MW — minimum 2%.

Conclusion

As a result of the study, it is shown that from the point of view of ICR heating in modes with a small additive (hydrogen or helium-3), the Globus-M2 spherical tokamak is characterized by large values of the parameter ξ (3), which is equivalent to a high absorption density of high frequency energy. This circumstance may limit the opportunity of increasing the input power, since it leads to the appearance of poorly retained high-energy ions. For example, for the three-ion scenario already at a low power of 200 kW and ^{3}He concentrations of 1%, most particles obtain energy outside the confined band of 80 keV characteristic of Globus-M2. The energy of particles accelerated in ion cyclotron resonance decreases with increasing their density, however, in this case, the specific power absorbed per unit plasma volume may decrease due to a decrease in the polarization amplitude of the FMS wave rotating together with ions ^{3} He. However, it should be noted that experiments on high frequency heating at Globus-M show that with an increase in the concentration of a small additive of hydrogen in a spherical tokamak, the heating efficiency can be maintained and thus represent a way to solve the specified problem. A similar effect can also be expected for the three-ion scenario. At relative ^{3}He concentrations of approximately 2 to 7% and high plasma concentrations, most of the accelerated particles can be kept in a tokamak at the pumping power available on Globus-M2.

Acknowledgments

The studies presented in Section 1 were carried out as part of state task 0040-2019-0023 of the Physicotechnical Institute named after A.F. Ioffe, while the studies presented in Section 2 were carried out as part of state task 0034-2021-0002 of the Physicotechnical Institute named after A.F. Ioffe.

Conflict of interest

The authors declare that they have no conflict of interest.

References

[1] J. Wesson. *Tokamaks* (Clarendon press, Oxford, 2004)
[2] J. Adam. Plasma Phys. Control. Fusion, **29**, 443 (1987). DOI: 10.1088/0741-3335/29/4/001
[3] V.E. Golant, V.I. Fedorov. *High-Frequency Methods for Plasma Heating in Toroidal Thermonuclear Devices* (Ehnergoatomizdat, M. (USSR), 1986)
[4] V.K. Gusev, V.V. D'yachenko, F.V. Chernyshev, Yu.V. Petrov, N.V. Sakharov, O.N. Shcherbinin, Tech. Phys. Lett., **30**, 8, 690 (2004). DOI: 10.1134/1.1792315
[5] Yu. Yang, X. Zhang, Y. Zhao, Ch. Qin, Y. Cheng, Yu. Mao, H. Yang, J. Wang, Sh. Yuan, L. Wang, S. Ju, G. Chen, Xu Deng, K. Zhang, B. Wan, J. Li , Yu. Song, X. Gong, J. Qian, T. Zhang. Plasma Sci. Tech., **20**, 045102 (2018). DOI: 10.1088/2058-6272/aaa599
[6] M. Saigusa, H. Kimura, S. Moriyama, Y. Neyatani, T. Fujii, Y. Koide, T. Kondoh, M. Sato, M. Nemoto, Y. Kamada. Plasma Phys. Control. Fusion, **37**, 295 (1995). DOI: 10.1088/0741-3335/37/3/009
[7] V.P. Bhatnagar, J. Jacquinto, D.F.H. Start, B.J.D. Tubbing. Nucl. Fusion, **33**, 83 (1993). DOI: 10.1088/0029-5515/33/1/I08
[8] A.M. Messiaen, D. Van Eester, R. Koch, J. Ongena, G. Van Wassenhove, R.R. Weynants, P. Borgermans, H. Conrads, P. Dumortier, F. Durodie, G. Fuchs, H. Euringer, B. Giesen, D. Hillis, F. Hoenen, H.R. Koslowski, A. Kramer-Flecken, M. Lochter, T. Oyevaar, H. Soltwisch, H.F. Tammen, G. Telesca, R. Uhlemann, L. Van Den Durpel, P.E. Vandenplas, R. Van Nieuwenhove, G. Van Oost, M. Vervier, G. Waidmann. Plasma Phys. Control. Fusion, **32**, A15 (1993). DOI: 10.1088/0741-3335/35/SA/002
[9] K. Steinmetz, H. Niedermeyer, J.-M. Noterdaeme, F. Wagner, F. Wesner, J. Bäumler, G. Becker, W. Becker, H.S. Bosch, M. Brambilla. Nucl. Fusion, **29**, 277 (1989). DOI: 10.1088/0029-5515/29/2/010
[10] E.J. Synakowski, M.G. Bell, R.E. Bell, T. Bigelow, M. Bitter, W. Blanchard, J. Boedo, C. Bourdelle, C. Bush, D.S. Darrow, P.C. Efthimion, E.D. Fredrickson, D.A. Gates M. Gilmore, L.R. Grisham, J.C. Hosea, D.W. Johnson, R. Kaita, S.M. Kaye, S. Kubota, H.W. Kugel, B.P. LeBlanc, K. Lee, R. Maingi, J. Manickam, R. Maqueda, E. Mazzucato, S.S. Medley, J. Menard, D. Mueller, B.A. Nelson, C. Neumeyer, M. Ono, F. Paoletti, H.K. Park, S.F. Paul, Y.-K.M. Peng, C.K. Phillips, S. Ramakrishnan, R. Raman, A.L. Roquemore, A. Rosenberg, P.M. Ryan, S.A. Sabbagh, C.H. Skinner, V. Soukhanovskii, T. Stevenson, D. Stutman, D.W. Swain, G. Taylor, A. Von Halle, J. Wilgen, M. Williams, J.R. Wilson, S.J. Zweben, R. Akers, R.E. Barry, P. Beiersdorfer, J.M. Bialek, B. Blagojevic, P.T. Bonoli, R. Budny, M.D. Carter, C.S. Chang, J. Chrzanowski, W. Davis, B. Deng, E.J. Doyle, L. Dudek, J. Egedal, R. Ellis, J.R. Ferron, M. Finkenthal, J. Foley, E. Fredd, A. Glasser, T. Gibney, R.J. Goldston, R. Harvey, R.E. Hatcher, R.J. Hawryluk, W. Heidbrink, K.W. Hill, W. Houlberg, T.R. Jarboe, S.C. Jardin, H. Ji, M. Kalish, J. Lawrance, L.L. Lao, K.C. Lee, F.M. Levinton, N.C. Luhmann, R. Majeski, R. Marsala, D. Mastravito, T.K. Mau, B. McCormack, M.M. Menon, O. Mitarai, M. Nagata, N. Nishino, M. Okabayashi, G. Oliaro, D. Pacella, R. Parsells, T. Peebles, B. Peneflor, D. Piglowski, R. Pinsker, G.D. Porter, A.K. Ram, M. Redi, M. Rensink, G. Rewoldt, J. Robinson, P. Roney, M. Schaffer, K. Shaing, S. Shiraiwa, P. Sichta, D. Stotler, B.C. Stratton, Y. Takase, X. Tang, R. Vero, W.R. Wampler, G.A. Wurden, X.Q. Xu, J.G. Yang, L. Zeng, W. Zhu. Nucl. Fusion, **43**, 1653 (2003). DOI: 10.1088/0029-5515/43/12/011

[11] D.A. Gates, J. Ahn, J. Allain, R. Andre, R. Bastasz, M. Bell, R. Bell, E. Belova, J. Berkery, R. Betti, J. Bialek, T. Biewer, T. Bigelow, M. Bitter, J. Boedo, P. Bonoli, A. Boozer, D. Brennan, J. Breslau, D. Brower, C. Bush, J. Canik, G. Caravelli, M. Carter, J. Caughman, C. Chang, W. Choe, N. Crocker, D. Darrow, L. Delgado-Aparicio, S. Diem, D. D'Ippolito, C. Domier, W. Dorland, P. Efthimion, A. Ejiri, N. Ershov, T. Evans, E. Feibush, M. Fenstermacher, J. Ferron, M. Finkenthal, J. Foley, R. Frazin, E. Fredrickson, G. Fu, H. Funaba, S. Gerhardt, A. Glasser, N. Gorelenkov, L. Grisham, T. Hahm, R. Harvey, A. Hassanein, W. Heidbrink, K. Hill, J. Hillesheim, D. Hillis, Y. Hirooka, J. Hosea, B. Hu, D. Humphreys, T. Idehara, K. Indireshkumar, A. Ishida, F. Jaeger, T. Jarboe, S. Jardin, M. Jaworski, H. Ji, H. Jung, R. Kaita, J. Kallman, O. Katsuro-Hopkins, K. Kawahata, E. Kawamori, S. Kaye, C. Kessel, J. Kim, H. Kimura, E. Kolemen, S. Krasheninnikov, P. Krstic, S. Ku, S. Kubota, H. Kugel, R. La Haye, L. Lao, B. LeBlanc, W. Lee, K. Lee, J. Leuer, F. Levinton, Y. Liang, D. Liu, N. Luhmann Jr, R. Maingi, R. Majeski, J. Manickam, D. Mansfield, R. Maqueda, E. Mazzucato, D. McCune, B. McGeehan, G. McKee, S. Medley, J. Menard, M. Menon, H. Meyer, D. Mikkelsen, G. Miloshevsky, O. Mitarai, D. Mueller, S. Mueller, T. Munsat, J. Myra, Y. Nagayama, B. Nelson, X. Nguyen, N. Nishino, M. Nishiura, R. Nygren, M. Ono, T. Osborne, D. Pacella, H. Park, J. Park, S. Paul, W. Peebles, B. Penaflor, M. Peng, C. Phillips, A. Pigarov, M. Podesta, J. Preinhaelter, A. Ram, R. Raman, D. Rasmussen, A. Redd, H. Reimerdes, G. Rewoldt, P. Ross, C. Rowley, E. Ruskov, D. Russell, D. Ruzic, P. Ryan, S. Sabbagh, M. Schaffer, E. Schuster, S. Scott, K. Shaing, P. Sharpe, V. Shevchenko, K. Shinohara, V. Sizyuk, C. Skinner, A. Smirnov, D. Smith, S. Smith, P. Snyder, W. Solomon, A. Sontag, V. Soukhanovskii, T. Stoltzfus-Dueck, D. Stotler, T. Strait, B. Stratton, D. Stutman, R. Takahashi, Y. Takase, N. Tamura, X. Tang, G. Taylor, C. Taylor, C. Ticos, K. Tritz, D. Tsarouhas, A. Turrnbull, G. Tynan, M. Ulrickson, M. Umansky, J. Urban, E. Utergberg, M. Walker, W. Wampler, J. Wang, W. Wang, A. Welander, J. Whaley, R. White, J. Wilgen, R. Wilson, K. Wong, J. Wright, Z. Xia, X. Xu, D. Youchison, G. Yu, H. Yuh, L. Zakharov, D. Zemlyanov, S. Zweben. Nucl. Fusion, **49**, 104016 (2009). DOI: 10.1088/0029-5515/49/10/104016

[12] H. Meyer, I.G. Abel, R.J. Akers, A. Allan, S.Y. Allan, L.C. Appel, O. Asunta, M. Barnes,, N.C. Barratt, N. Ben Ayed, J.W. Bradley, J. Canik, P. Cahyna, M. Cecconello, C.D. Challis, I.T. Chapman, D. Ciric, G. Colyer, N.J. Conway, M. Cox, B.J. Crowley, S.C. Cowley, G. Cunningham, A. Danilov, A. Darke, M.F.M. De Bock, G. De Temmerman, R.O. Dendy, P. Denner, D. Dickinson, A.Y. Dnestrovsky, Y. Dnestrovsky, M.D. Driscoll, B. Dudson, D. Dunai, M. Dunstan, P. Dura, S. Elmore, A.R. Field, G. Fishpool, S. Freethy, W. Fundamenski, L. Garzotti, Y.C. Ghim,, K.J. Gibson, M.P. Gryaznevich, J. Harrison, E. Havlíčková, N.C. Hawkes, W.W. Heidbrink, T.C. Hender, E. Highcock, D. Higgins, P. Hill, B. Hnat, M.J. Hole, J. Horek, D.F. Howell, K. Imada, O. Jones, E. Kaveeva, D. Keeling, A. Kirk, M. Kočan, R.J. Lake, M. Lehnen, H.J. Leggate, Y. Liang, M.K. Lilley, S.W. Lisgo, Y.Q. Liu, B. Lloyd, G.P. Maddison, J. Mailloux, R. Martin, G.J. McArdle, K.G. McClements, B. McMillan, C. Michael, F. Militello, P. Molchanov, S. Mordijck, T. Morgan, A.W. Morris, D.G. Muir, E. Nardon, V. Naulin, G. Naylor, A.H. Nielsen, M.R. O'Brien, T. O'Gorman, S. Pamela, F.I. Parra, A. Patel, S.D. Pinches, M.N. Price, C.M. Roach, J.R. Robinson, M. Romanelli, V. Rozhansky, S. Saarelma, S. Sangaroon, A. Saveliev, R. Scannell, J. Seidl, S.E. Sharapov, A.A. Schekochihin, V. Shevchenko, S. Shibaev, D. Stork, J. Storrs, A. Sykes, G.J. Tallents, P. Tamain, D. Taylor, D. Temple, N. Thomas-Davies, A. Thornton, M.R. Turnyanskiy, M. Valovič, R.G.L. Vann, E. Verwichte, P. Voskoboynikov, G. Voss, S.E.V. Warder, H.R. Wilson, I. Wodniak, S. Zoletnik, R. Zagôrski and the MAST and NBI Teams. Nucl. Fusion, **53**, 104008 (2013). DOI: 10.1088/0029-5515/53/10/104008

[13] B. Lloyd, R.J. Akers, F. Alladio, S. Allan, L.C. Appel, M. Barnes, N.C. Barratt, N. Ben Ayed, B.N. Breizman, M. Cecconello, C.D. Challis, I.T. Chapman, D. Ciric, G. Colyer, J.W. Connor, N.J. Conway, M. Cox, S.C. Cowley, G. Cunningham, A. Darke, M. De Bock, E. Delchambre, G. De Temmerman, R.O. Dendy, P. Denner, M.D. Driscoll, B. Dudson, D. Dunai, M. Dunstan, S. Elmore, A.R. Field, G. Fishpool, S. Freethy, L. Garzotti, K.J. Gibson, M.P. Gryaznevich, W. Guttenfelder0, J Harrison, R.J. Hastie, N.C. Hawkes, T.C. Hender, B. Hnat, D.F. Howell, M.-D. Hua, A. Hubbard, G. Huysmans, D. Keeling, Y.C. Kim, A. Kirk, Y. Liang, M.K. Lilley, M. Lisak, S. Lisgo, Y.Q. Liu, G.P. Maddison, R. Maingi, S.J. Manhood, R. Martin, G.J. McArdle, J. McCone, H. Meyer, C. Michael, S. Mordijck, T. Morgan, A.W. Morris, D.G. Muir, E. Nardon, G. Naylor, M.R. O'Brien, T. O'Gorman, J. Páleník, A. Patel, S.D. Pinches, M.N. Price, C.M. Roach, V. Rozhansky, S. Saarelma, S.A. Sabbagh, A. Saveliev, R. Scannell, S.E. Sharapov, V. Shevchenko, S. Shibaev, D. Stork, J. Storrs, W. Suttrop, A. Sykes, P. Tamain, D. Taylor, D. Temple, N. Thomas-Davies, A. Thornton, M.R. Turnyanskiy, M. Valovic, R.G.L. Vann, G. Voss, M.J. Walsh, S.E.V. Warder, H.R. Wilson, M. Windridge, M Wisse, S. Zoletnik and the MAST and NBI teams. Nucl. Fusion, **51**, 094013 (2011). DOI: 10.1088/0029-5515/51/9/094013

[14] V.B. Minaev, V.K. Gusev, N.V. Sakharov, Yu.V. Petrov, V.I. Varfolomeev, F.V. Chernyshev, N.N. Bakharev, V.V. Dyachenko, N.A. Khromov, G.S. Kurskiev, A.B. Mineev, V.A. Rozhansky, A.N. Saveliev, P.B. Shchegolev, I.V. Shikhovtsev. EPJ Web Conf., **149**, 03001 (2017). DOI: 10.1051/epjconf/201714903001

[15] N.N. Bakharev, G.I. Abdullina, V.I. Afanasyev, A.B. Altukhov, L.G. Askinazi, N.A. Babinov, A.N. Bazhenov, A.A. Belokurov, M.D. Blekhshtein, E.N. Bondarchuk, I.M. Bukreev, V.V. Bulanin, An.P. Chernakov, F.V. Chernyshev, I.N. Chugunov, A.M. Dmitriev, D.N. Doinikov, V.V. Dyachenko, L.A. Esipov, D.B. Gin, A.V. Gorbunov, A.D. Gurchenko, E.Z. Gusakov, V.K. Gusev, S. Heuraux, M.V. Iliasova, M.A. Irzak, S.N. Kamenshikov, A.A. Kavin, E.M. Khilkevitch, N.A. Khromov, E.O. Kiselev, T.P. Kiviniemi, A.A. Kobelev, V.A. Kornev, A.N. Koval, D.V. Kouprienko, S.V. Krikunov, O.L. Krutkin, G.S. Kurskiev, S.I. Lashkul, S.V. Lebedev, C. Lechte, S. Leerink, A.E. Litvinov, K.M. Lobanov, S.V. Masyukevich, A.A. Martynov, S.Yu. Medvedev, A.D. Melnik, V.B. Minaev, A.B. Mineev, M.I. Mironov, I.V. Miroshnikov, E.E. Mukhin, V.O. Naidenov, A.S. Navolotsky, V.G. Nesenevich, P. Niskala, A.N. Novokhatskii, K.Yu. Oshuev, M.I. Patrov, A.V. Petrov, M.P. Petrov, S.Ya. Petrov, Yu.V. Petrov, I.A. Polunovsky, A.Yu. Popov, A.G. Razdobarin, D.V. Razumenko, V.V. Rozhdestvensky, N.V. Sakharov, D.S. Samsonov, A.N. Saveliev, V.A. Senichenkov, P.B. Shchegolev, A.E. Shevelev,

A.D. Sladkomedova, A.I. Smirnov, A.S. Smirnov, V.V. Solokha, V.A. Solovei, A.Yu. Stepanov, A.Yu. Telnova, V.A. Tokarev, S.Yu. Tolstyakov, P.V. Tretinnikov, I.B. Tereschenko, A.S. Tukachinsky, E.A. Tukhmeneva, V.I. Varfolomeev, L.A. Varshavchick, A.Yu. Yashin, E.G. Zhilin, N.A. Zhubr. Nucl. Fusion, **59**, 112022 (2019). DOI: 10.1088/1741-4326/ab22dc

[16] G.S. Kurskiev, N.N. Bakharev, V.V. Bulanin, F.V. Chernyshev, V.K. Gusev, N.A. Khromov, E.O. Kiselev, V.B. Minaev, I.V. Miroshnikov, E.E. Mukhin, M.I. Patrov, A.V. Petrov, Yu.V. Petrov, N.V. Sakharov, P.B. Shchegolev, A.D. Sladkomedova, V.V. Solokha, A.Yu. Telnova, S.Yu. Tolstyakov, V.A. Tokarev, A.Yu. Yashin. Nucl. Fusion, **59**, 066032 (2019). DOI: 10.1088/1741-4326/ab15c5

[17] M. Gryaznevich. Tokamak Energy team. AIP Conf. Proc., **2179**, 020008 (2019). DOI: 10.1063/1.5135481

[18] M. Gryaznevich, O. Asunta. Tokamak Energy Ltd Team. Fusion Eng. Des., **123**, 177 (2017). DOI: 10.1016/j.fusengdes.2017.03.011

[19] M. Gryaznevich, R. Akers, P.G. Carolan, N.J. Conway, D. Gates, A.R. Field, T.C. Hender, I. Jenkins, R. Martin, M.P.S. Nightingale, C. Ribeiro, D.C. Robinson, A. Sykes, M. Tournianski, M. Valovič, M.J. Walsh. Phys. Rev. Lett., **80**, 3972 (1998). DOI: 10.1103/PhysRevLett.80.3972

[20] Ye.O. Kazakov, D. Van Eester, R. Dumont, J. Ongena. Nucl. Fusion, **55**, 032001 (2015). DOI: 10.1088/0029-5515/55/3/032001

[21] V.K. Gusev, F.V. Chernyshev, V.V. Dyachenko, Yu.V. Petrov, N.V. Sakharov, V.L. Vdovin, O.N. Shcherbinin. *ICRH Experiments on the Spherical Tokamak Globus-M*. EX/5-6. Proceedings of the 20th IAEA Fusion Energy Conference, 1–6 November, 2004, Vilamoura, Portugal.

[22] O.N. Shcherbinin, F.V. Chernyshev, V.V. Dyachenko, V.K. Gusev, Yu.V. Petrov, N.V. Sakharov, V.M. Leonov. Nucl. Fusion, **46**, S592 (2006). DOI: 10.1088/0029-5515/46/8/S04

[23] V.V. Dyachenko, B.B. Ayushin, V.K. Gusev, S.A. Khitrov, F.V. Chernyshev, M.I. Mironov, Yu.V. Petrov, N.V. Sakharov, O.N. Shcherbinin. AIP Conf. Proceed., **1187**, 197 (2009). DOI: 10.1063/1.3273726

[24] F.V. Chernyshev, B.B. Ayushin, V.K. Gusev, V.V. D'yachenko, V.B. Minaev, M.I. Mironov, M.P. Petrov, Yu.V. Petrov, N.V. Sakharov, S.A. Khitrov, O.N. Shcherbinin. Plasma Phys. Rep., **35** (11), 903 (2009). DOI: 10.1134/S1063780X09110014

[25] Ye.O. Kazakov, J. Ongena, J.C. Wright, S.J. Wukitch, V. Bobkov, J. Garcia, V.G. Kiptily, M. J. Mantsinen, M. Nocente, M. Schneider, H. Weisen, Y. Baranov, M. Baruzzo, R. Bilato, A. Chomiczewska, R. Coelho, T. Craciunescu, K. Crombé, M. Dreval, R. Dumont, P. Dumortier, F. Durodié, J. Eriksson, M. Fitzgerald, J. Galdon-Quiroga, D. Gallart, M. Garcia-Muñoz, L. Giacomelli, C. Giroud, J. Gonzalez-Martin, A. Hakola, P. Jacquet, T. Johnson, A.Kappatou, D.Keeling, D.King, K.K. Kirov, P. Lamalle, M. Lennholm, E. Lerche, M. Maslov, S. Mazzi, S. Menmuir, I. Monakhov, F. Nabais, M. F. F. Nave, R. Ochoukov, A. R. Polevoi, S. D. Pinches, U. Plank3, D. Rigamonti, M. Salewski, P. A. Schneider, S. E. Sharapov, Ž. Štancar, A. Thorman, D. Valcarcel5, D. Van Eester1, M. Van Schoor1, J. Varje, M. Weiland, N. Wendler, JET Contributors, ASDEX Upgrade Team, EUROfusion MST1 Team and Alcator C-Mod Team. Phys. Plasmas, 28, 020501 (2021). DOI: 10.1063/5.0021818

[26] Ye.O. Kazakov, D. Van Eester, R. Dumont, J. Ongena. Nucl. Fusion, **55**, 032001 (2015). DOI: 10.1088/0029-5515/55/3/032001

[27] J.M. Faustin, J.P. Graves, W.A. Cooper, S. Lanthaler, L. Villard, D. Pfefferlé, J. Geiger, Ye O. Kazakov, D. Van Eester. Plasma Phys. Control. Fusion, **59** (8), 084001 (2017). DOI: 10.1088/1361-6587/aa72a4

[28] Ye.O. Kazakov, I.V. Pavlenko, D. Van Eester, B. Weyssow, I.O. Girka. Plasma Phys. Control. Fusion, **52**, 115006 (2010). DOI: 10.1088/0741-3335/52/11/115006

[29] F.W. Perkins. Nucl. Fusion, **17**, 1197 (1977). DOI: 10.1088/0029-5515/17/6/008

[30] M. Brambilla. Plasma Phys. Control. Fusion, **31**, 723 (1989). DOI: 10.1088/0741-3335/31/5/004

[31] G.S. Kurskiev, V.K. Gusev, N.V. Sakharov, N.N. Bakharev, A.D. Iblyaminova, P.B. Shchegolev, G.F. Avdeeva, E.O. Kiselev, V.B. Minaev, E.E. Mukhin, M.I. Patrov, Yu.V. Petrov, A.Yu. Telnova, S.Yu. Tolstyakov. Plasma Phys. Control. Fusion, **59**, 045010 (2017). DOI: 10.1088/1361-6587/aa5cd5

[32] K. Appert, T. Hellsten, J. Vaclavik, L. Villard. Comp. Phys. Commun., **40**, 73 (1986). DOI: 10.1016/0010-4655(86)90149-9

[33] T.H. Stix. Nucl. Fusion, **15**, 737 (1975). DOI: 10.1088/0029-5515/15/5/003

[34] J. Hosea, S. Bernabei, P. Colestock, S.L. Davis, P. Efthimion, R.J. Goldston, D. Hwang, S.S. Medley, D. Mueller, J. Strachan, H. Thompson. Phys. Rev. Lett., **43** (24), 1802 (1979). DOI: 10.1103/PhysRevLett.43.1802

[35] A.B. Izvozchikov, M.P. Petrov, S.Ya. Petrov, F.V. Chernyshev, I.V. Shustov. Tech. Phys., **37** (2), 201 (1992).]